Saudi Journal of Biological Sciences 27 (2020) 1251–1259

Contents lists available at ScienceDirect

Saudi Journal of Biological Sciences

journal homepage: www.sciencedirect.com

Original article

The role of activated NLRP3 inflammatory body in acute kidney injury in rats caused by sepsis and NLRP3-TXNIP signaling pathway

Huanghao Deng, Fangzhi Chen, Yinhuai Wang, Hongyi Jiang, Zhitao Dong, Biao Yuan, Xiaokun Zhao *

Department of Urology, The Second Xiangya Hospital, Central South University, Changsha, Hunan 410011, China

ARTICLE INFO

Article history:
Received 13 January 2020
Revised 29 February 2020
Accepted 8 March 2020
Available online 18 March 2020

Keywords:
NLRP3 inflammatory corpuscles
Abdominal resection by surgical suture
Acute kidney injury
NLRP3-TXNIP signaling pathway

ABSTRACT

Objective: The model of acute renal injury (AKI) induced by sepsis in rats was established by abdominal resection through surgical suture. The activation mechanism of nod-like receptor with pyrin domain containing 3 (NLRP3) inflammatory corpuscle in AKI induced by sepsis was analyzed.
Methods: Here, 60 male rats were selected and divided into two groups, including sham-operated group (NO-OPs group, n = 15) and sepsis group (CELP group, n = 45). In order to examine each index of CELP group, four time points (10, 20, 30, and 40 h) were set as control. In NO-OPs group, only abdominal resection through surgical suture was carried out. The expression levels of NLRP3, apoptosis-associated speck-like protein containing a C-terminal caspase recruitment domain (ASC), caspase-1, and the expression level of NLRP3-TXNIP signaling pathway were measured by immunohistochemistry, Western blotting, immunoprecipitation, and mito-TEMPO (a mitochondria-targeted antioxidant) 40 h after operation and 10, 20, 30, and 40 h post-operation in CELP group. Herein, 40 h post-operation in NO-OPs group and 10, 20, 30, and 40 h post-operation in CELP group, peripheral blood samples were collected.
Results: Compared with NO-OPs group, the levels of serum creatinine (Scr) and blood urea nitrogen (BUN) in CELP group were increased ($P < 0.05$). Compared with NO-OPs group, the expression levels of interleukin-1β (IL-1β), NLRP3, ASC, and caspase-1 in CELP group were increased ($P < 0.05$). The expression level of TXNIP in renal tubular epithelial cells in rats was up-regulated. There was a positive correlation between TXNIP and NLRP3. The binding of NLRP3-TXNIP signaling pathway could be inhibited by siRNA transfection or mito-TMPO, and the activity of NLRP3 inflammatory bodies could be inhibited as well.
Conclusion: Activation of NLRP3 inflammatory corpuscles could promote AKI induced by sepsis. Simultaneously, renal injury may lead to the production of mitochondrial reactive oxygen species (mROS), which may induce the binding of TXNIP to NLRP3.

1. Introduction

Sepsis is a comprehensive inflammation caused by bacterial infection, and that is mainly accompanied by shock and organ dysfunction, as well as several other complications Zhang et al. (2012). Among them, sepsis-induced acute kidney injury is a kind of complication with high frequency, and the current treatment for this complication needs to be further improved. When microorganisms infect humans, blood-borne lipopolysaccharide (LPS) supplies a large amount of blood. This phenomenon may be recognized by the cell membrane pattern of neutrophils and macrophages, that may stimulate downstream signals, produce a great number of inflammatory mediators, promote immune cells to prevent inflammation, and then lead to a serious deficiency related to immune cells in other organs of the kidney, directly causing damage to these organs Young et al. (2018).

A study showed that the damage to tubular epithelial cells is a key factor in the development of acute kidney injury (AKI) when kidney injury or AKI occurs. When the kidney is damaged or confronted with viral material tools, renal tubular epithelial cells Craciun et al. (2014), as a protective layer of the kidney, are extremely vulnerable to damage and fall off into the lumen, leading to renal tubular necrosis. Mitochondria are the main source of energy for cells, playing a substantial role in the whole cell activity. Khwaja and Arif (2012) demonstrated that the mitochondrial

* Corresponding author at: Department of Urology, The Second Xiangya Hospital, Central South University, No. 139 Renmin Road, Changsha, Hunan 410011, China.
E-mail address: zhaoxiaokunyeah@yeah.net (X. Zhao).
Peer review under responsibility of King Saud University.

Production and hosting by Elsevier

https://doi.org/10.1016/j.sjbs.2020.03.018
1319-562X/

density decreases in mice with renal function damage. Correspondingly, the overall morphology of renal tubules may further develop towards malignancy, indicating that there is a significant correlation between mitochondria and AKI disease. Ostermann et al. (2012) reported that mitochondria and nitric oxide enzymes could produce a great number of mitochondrial reactive oxygen species (mROS) during the study of kidney injury, while there were no data to prove that mROS might cause damage to kidney tissues. Among all kinds of inflammatory reactions caused by kidney injury, nod-like receptor with pyrin domain containing 3 (NLRP3) inflammatory corpuscle may appear in large quantities and induce up-regulation of NLRP3, Caspase-1 (Inna et al., 2017; Bingbing et al., 2015; Satoh et al., 2014), interleukin-1β (IL-1β), interleukin-18 (IL-18), and other genes. Mccullough et al. (2016) demonstrated that reducing the expression of NLRP3 gene can attenuate the degree of renal tubular injury. There is a signaling pathway in the expression of NLRP3 gene. It has been reported that Thioredoxin-interacting protein (TXNIP) can regulate the activity of NLRP3 inflammatory bodies Jianru et al. (2015). In this study, the expression levels of NLRP3, C-terminal caspase recruitment domain (ASC), caspase-1 and NLRP3-TXNIP signaling pathway are detected by immunohistochemistry, Western blotting, immunoprecipitation and other methods based on the rat model of sepsis with acute renal injury. mito TEMPO is used for staining. The results are compared with those of rats who only have abdominal suture. The effect of NLRP3 on AKI and the mechanism of mROS - (TXNIP/NLRP3) signaling pathway on NLRP3 are studied.

2. Materials and methods

2.1. Subjects

In this study, 60 specific pathogen free (SPF) grade healthy male rats (body weight, 200–300 g) were selected and were randomly divided into two groups: sham-operated group (NO-OPs group, n = 20) and sepsis group (CELP group, n = 40). In order to test each index of CELP group, four time points (10, 20, 30, and 40 h) were set up. As control group, abdominal resection by surgical suture was performed only in NO-OPs group. This study was approved by the ethics committee.

2.2. Acute renal injury models induced by sepsis in rats

Rats were only supplied with water pre-operation. The rats were anaesthetized by intraperitoneal injection of chloral hydrate. The rats were in supine position on the operating table. Blood samples were collected from the tail vein, and then centrifuged and stored. A small incision was excised in the middle of the abdomen, and the skin and mucosa were separated to obtain the cecum. The sepsis model of rats was established by abdominal resection through surgical suture (CELP). The cecum artery was ligated with needle (No. 10) at 1/2 of the end of the cecum, and the cecum artery was ligated with the surgical line (No. 4). The blood color was changed and the cecum was sutured and closed post-operation. The rats in NO-OPs group only underwent laparotomy, and the temperature was kept at room temperature during the experiment. After the operation, rats received a large amount of drinking water. Caesarean section causes tissue damage, cecal ligation causes tissue necrosis. After perforation, the intestinal contents mixed with bacteria flowed into the abdominal cavity of mice, causing infection, peritonitis and sepsis.

2.3. Kidney function and pathological analysis of rats

Blood samples were collected and sent to the laboratory for further analysis. A cutting-edge automatic biochemical analyzer was used to detect serum creatinine (Scr), in addition to blood urea nitrogen (BUN) levels. Pathological analysis of the kidney tissues after infection was carried out. Fixation of tissues was performed with 5% paraformaldehyde (PFA). Kidney tissues were sliced and dewaxed by dehydration, wax immersion, and embedding. Hematoxylin and eosin (H&E) staining was undertaken to stain the slices, and then the slices of the kidney were dehydrated twice. The slices were sealed with glass and placed under a microscope (magnification, 200×) to observe the morphology of cells.

2.4. Immunohistochemistry to detect the expression of NLRP3 and related proteins

The prepared slices of kidney tissues were dewaxed, and then placed in water. The brown-yellow areas in the slices were positive cells. The antigen repair solution was placed in a beaker and heated in a microwave oven. The slices were added to the repair solution and heated for 15 min, and then gradually cooled to room temperature. The sheets were immersed in phosphate-buffered saline (PBS) solution (Gibco, MA, USA), and the experiments were repeated for three times. The peroxidase activity was eliminated by 3% deionized water (BioTek Instruments, Inc., Winooski, VT, USA), the PBS solution was also used for cleaning, and the experiments were repeated for three times. Goat serum working fluid was added to the surface of the thin sheet and incubated at room temperature for 20 min. In addition, NRLP3, apoptosis-associated speck-like protein containing a C-terminal caspase recruitment domain (ASC), Caspase-1 (Abcam, Cambridge, UK), and IL-1β corresponding primary antibodies (Santa Cruz Biotechnology, Inc., Dallas, TX, USA) were mixed with PBS and placed on the surface of thin slices by dropping, so as to make it fully covered and stored at low temperature. PBS solution and protein labeling reagent were used to label the tissue. The optical densities of NRLP3, ASC, Caspase-1, and IL-1β were analyzed with Chemiluminescence Imaging and Analysis System (Azure Biosystems Inc., Dublin, CA, USA).

2.5. Detection of NLRP3/ASC/Caspase-1 p45/Caspase-1 P10 expression by immunoblotting

The obtained slices were placed in radioimmunoprecipitation assay (RIPA) buffer, then treated at low temperature, and further processed by low temperature plus centrifugation to obtain the extract containing protein. The concentration of the extract was analyzed as well. Bovine serum albumin (BSA) was used to classify the concentration, which was set as the standard of concentration, and then compared with the concentration of the extract. Preparation of polyacrylamide gel electrophoresis initially required cleaning the glass plate and proportioning according to a certain proportion of acute gel. The concentrated liquid was sealed, which needed to be unblocked in the electrophoresis operation. Simultaneously, the positive and negative electrodes were connected and adjusted to keep the current at 15 mA. The duration of electrophoresis was 2 h. The transfer of gel samples was then carried out. Besides, Tween-Tris-buffered saline (TTBS) was used for the allocation of skimmed milk powder, in which each gene in the antibody was diluted in a certain proportion, and then poured into the hybridization bag. Next, the samples in the bag were placed in TTBS for the second time of dilution. After dilution, they were packaged into polyvinylidene difluoride (PVDF) film and incubated at room temperature for 4 h.

The PVDF film was placed in TTBS, and TTBS was replaced during shaking. At this time, the film was liquid. The expression and luminescence intensity of each protein in the film were analyzed as well.

Table 1
Scr and BUN levels at different time points in each group (x ± s).

	Scr (μmol/l)	BUN (μmol/l)
NO-OPs-40 h	17.67 ± 4.38	3.88 ± 1.24
CELP-10 h	31.29 ± 7.36*#	5.88 ± 1.29
CELP-20 h	27.79 ± 6.47*#	7.48 ± 1.69*#
CELP-30 h	51.75 ± 11.78*	16.57 ± 3.88*
CELP-40 h	34.58 ± 8.18*#	8.23 ± 1.99*#

* *Compare of the current data with the data of NO-OPs-40 h group* ($P < 0.05$)
\# *Compare of the current data with the data of CELP-30 h group* ($P < 0.05$).

2.6. Western blotting

For Western blotting, polyacrylamide gel electrophoresis was used to detect the protein in the sample, react with the corresponding antibody, and react with the second antibody labeled with enzyme or isotope. The composition of protein was observed by positron-emission tomography (PET). Into each 1 mL of cold lysis buffer, 10 μl phosphatase inhibitor and 1 μl protease inhibitor were added. Solid tissues were placed in a Petri dish and divided into 2 mm * 2 mm pieces. A small amount of lysis buffer was added, stirred evenly, and then transferred to the centrifugal tube (Thermo Fisher Scientific, Waltham, MA, USA). The supernatant was removed. Then, it was transferred to a new cooling centrifuge tube to obtain the protein extract.

2.7. Hypoxia-reoxygenation injury models of renal tubular epithelial cells in rats

In this study, renal tubular epithelial cells were obtained from rats and hypoxia-reoxygenation injury (HRI) models were established. A sugar-free culture medium was placed in a three-gas incubator (Sanyo, Osaka, Japan) containing 90% N_2 and 10% CO_2. Cell culture medium containing renal tubular epithelial cells was transformed into sugar-free and anaerobic culture medium and placed in hypoxic environment for hypoxia. After treating hypoxia, the sugar-free and anaerobic culture medium was transformed into normal sugar-containing culture medium and placed in a normal incubator for re-oxygenation.

2.8. Cell siRNA transfection

The transfected cells were placed in 6 tubes in advance with Stealth siRNA NLRP3 HSS132812 and Stealth siRNA TXNIP HSS116391. Among them, 10 μl of RNAiMAX was added to tubes 1, 2, and 3, and 5 μl diluted RNA (4) or siRNA (5, 6) was added to tubes 4, 5, and 6, which were stirred evenly and then placed for 24 h.

2.9. Implementation of immunoprecipitation

After transfection, the cells were added into the cell lysis buffer, lysed at low temperature for 20 min, and then centrifuged to obtain the supernatant of the solution. A small amount of pyrolysis solution was used for Western blot analysis. After that, 15 μl of Protein A agarose beads were cleaned three times with pyrolysis buffer solution, and centrifuged after each cleaning. After immunoprecipitation, centrifugation was carried out at low temperature. At this time, the agarose beads were placed at the bottom of the tube, and the supernatant was removed. The agarose beads were then cleaned with pyrolysis solution and placed on the mass spectrometer for protein analysis.

2.10. Mitochondrial staining of renal tubular epithelial cells in rats

A hypersensitive kit was purchased from Fuzhou Maixin Biological Co., Ltd. (Fuzhou, China). It is an infrared fluorescence probe with

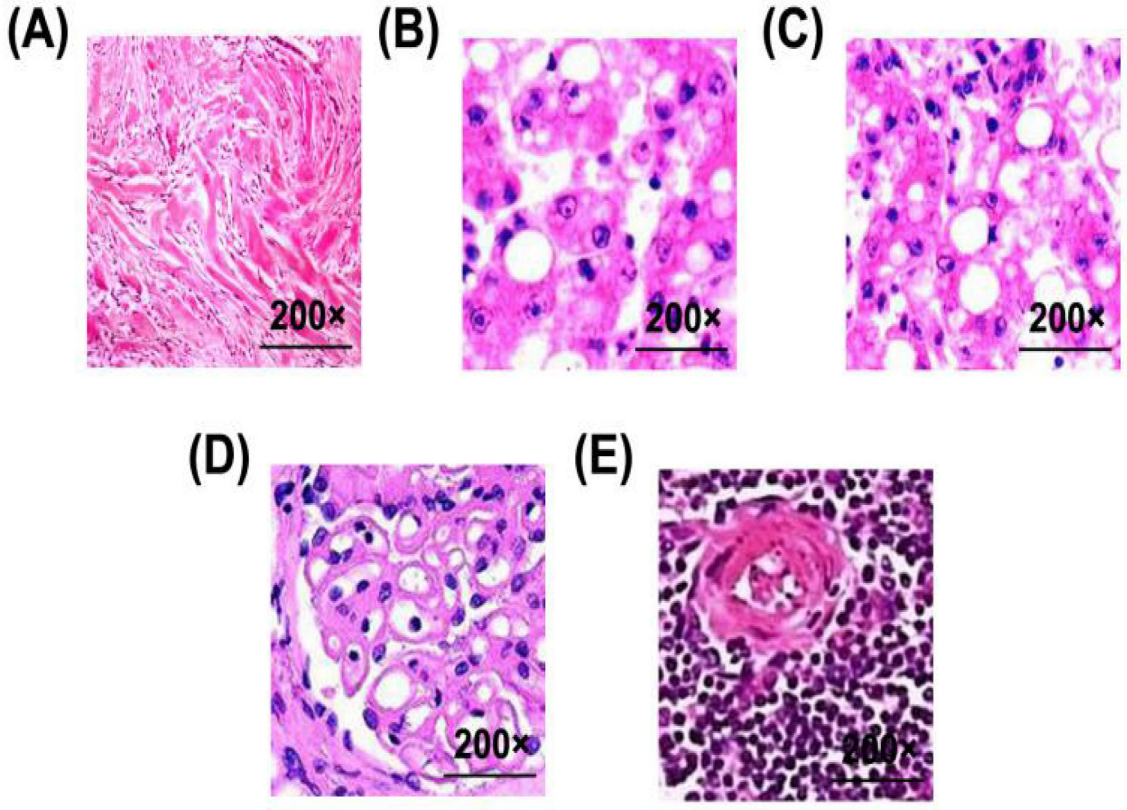

Fig. 1. Morphological changes of kidneys in rats stained with H&E. (A) 40 h after operation in NO-Ops group; (B) 10 h after operation in CELP group; (C) 20 h after operation in CELP group; (D) 30 h after operation in CELP group; (E) 40 h after operation in CELP group (magnification: 200×).

cell permeability, containing weak mercapto-reactive chloromethyl group in mitochondria. It can be aggregated on active mitochondria by simple cell culture. The fluorescent probes were added to anhydrous dimethyl sulfoxide (DMSO) for melting and cryopreservation to obtain the storage solution. Different probes were used according to different experimental purposes, and an appropriate buffer was added to produce different concentrations of working solution. The adherent cells of the culture medium were stained. The solution was centrifuged, and the supernatant was removed. Mito-Tracker Deep Red FM was used to stain the cells at 35 °C.

2.11. Statistical analysis

In this study, SPSS 21.0 software (IBM, Armonk, NY, USA) was used to analyze the test results of the two groups of rats. The data was expressed by x ± s, and the data of each group are compared by ANOVA. $P < 0.05$ has statistical significance, that is, there is significant difference between the two groups (see Table 1).

3. Results

3.1. Renal function

Compared with the sham-operated group (NO-OPs), the levels of Scr and BUN in CELP group tended to increase at 10 and 20 h ($P < 0.05$), which reached the highest level at 30 h post-operation. The levels of Scr and BUN in CELP group at 20 and 40 h post-operation were significantly different from those at 30 h after operation ($P < 0.05$).

3.2. Pathological results

In Fig. 1, Fig. 1A is the glomerular shape at 40 h post-operation in the sham-operated group. Fig. 1B–E shows the glomerular shape at different time points in CELP group. It is observed that with the prolongation of time, kidney epithelial cells and vacuoles appear in renal tissues after 40 h of sepsis.

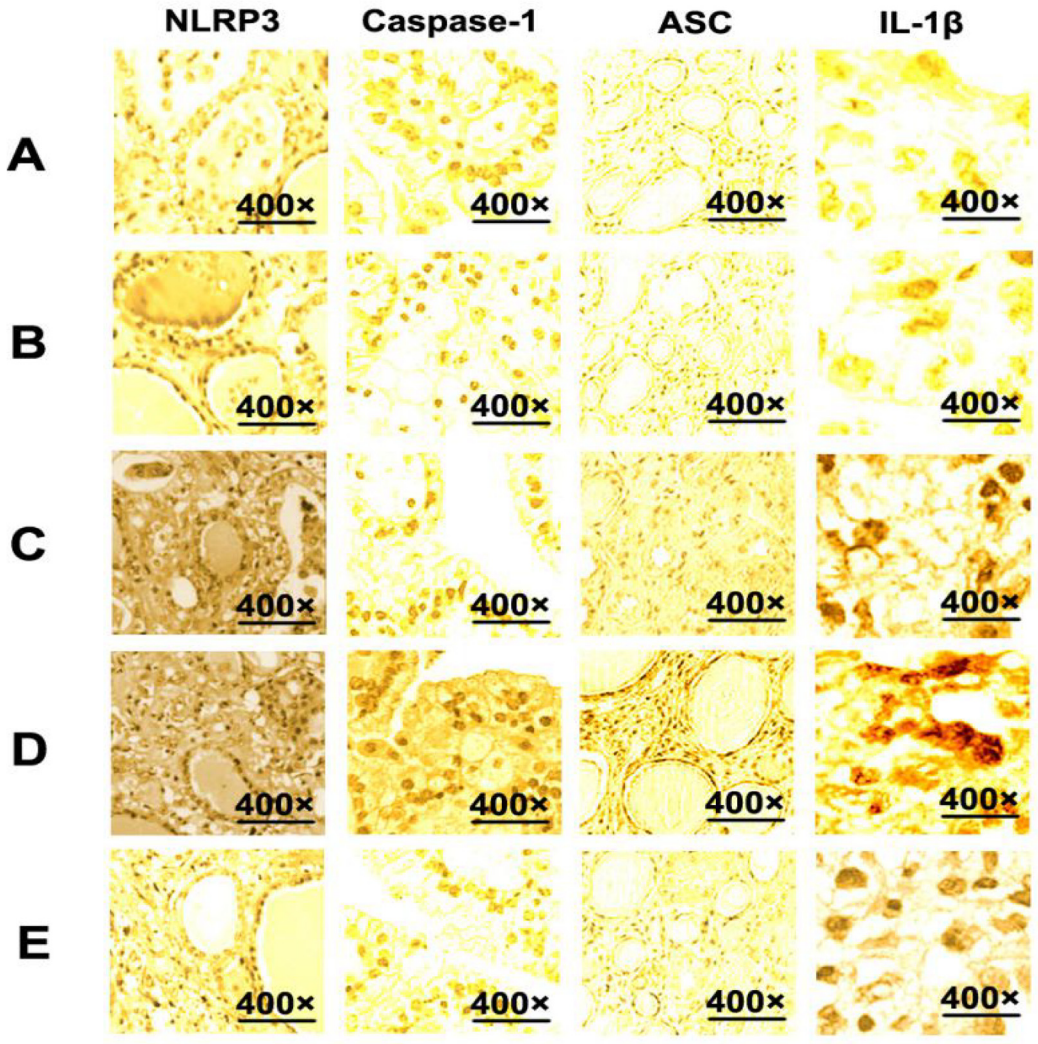

Fig. 2. The expression of NLRP3, ASC, Caspase-1, and IL-1β in kidney tissues of rats in each group. (A) 40 h after operation in NO-Ops group; (B) 10 h after operation in CELP group; (C) 20 h after operation in CELP group; (D) 30 h after operation in CELP group; (E) 40 h after operation in CELP group (magnification: 400×).

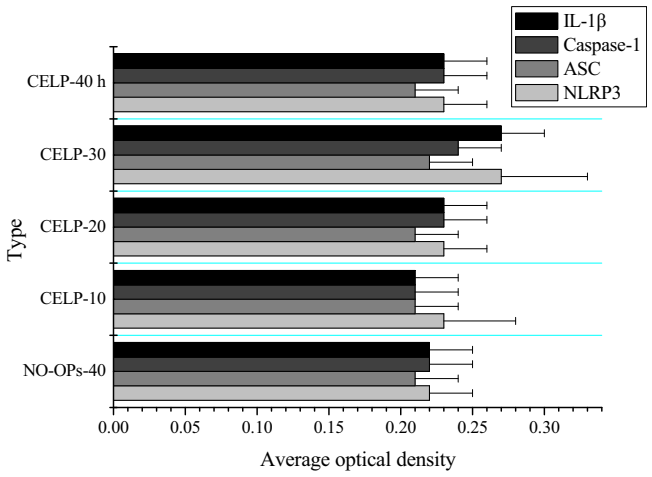

Fig. 3. Average optical densities of NLRP3, ASC, Caspase-1, and IL-1β (x ± s). *Compare of the current data with the data of NO-OPs-40 h group (*P* < 0.05).

3.3. Immunohistochemistry of NLRP3 and its related proteins in renal tissue

The average optical densities of NLRP3, ASC, Caspase-1 and IL-1β in kidney tissues at different time points were obtained by image analysis. As shown in Fig. 2, compared with sham-operated group, expression levels of Caspase-1, ASC, and IL-1β in renal tissues of CELP group increased 30 h after operation (P < 0.05). Besides, IL-1β and Caspase-1 were distributed in renal tubular epithelial cells (see Figs. 3 and 4).

3.4. Activity analysis of NLRP3 inflammatory bodies in renal tissues

The expression levels of NLRP3, ASC, Caspase-1, and IL-1β in renal tissues in different groups were detected by immunoblotting. The NLRP3, ASC, pro-caspase-1, cleaved-caspase-1, and glyceraldehyde 3-phosphate dehydrogenase (GAPDH) bands appeared at 110, 27, 45, 10, and 33 kDa, respectively. Compared with the NO-Ops group,

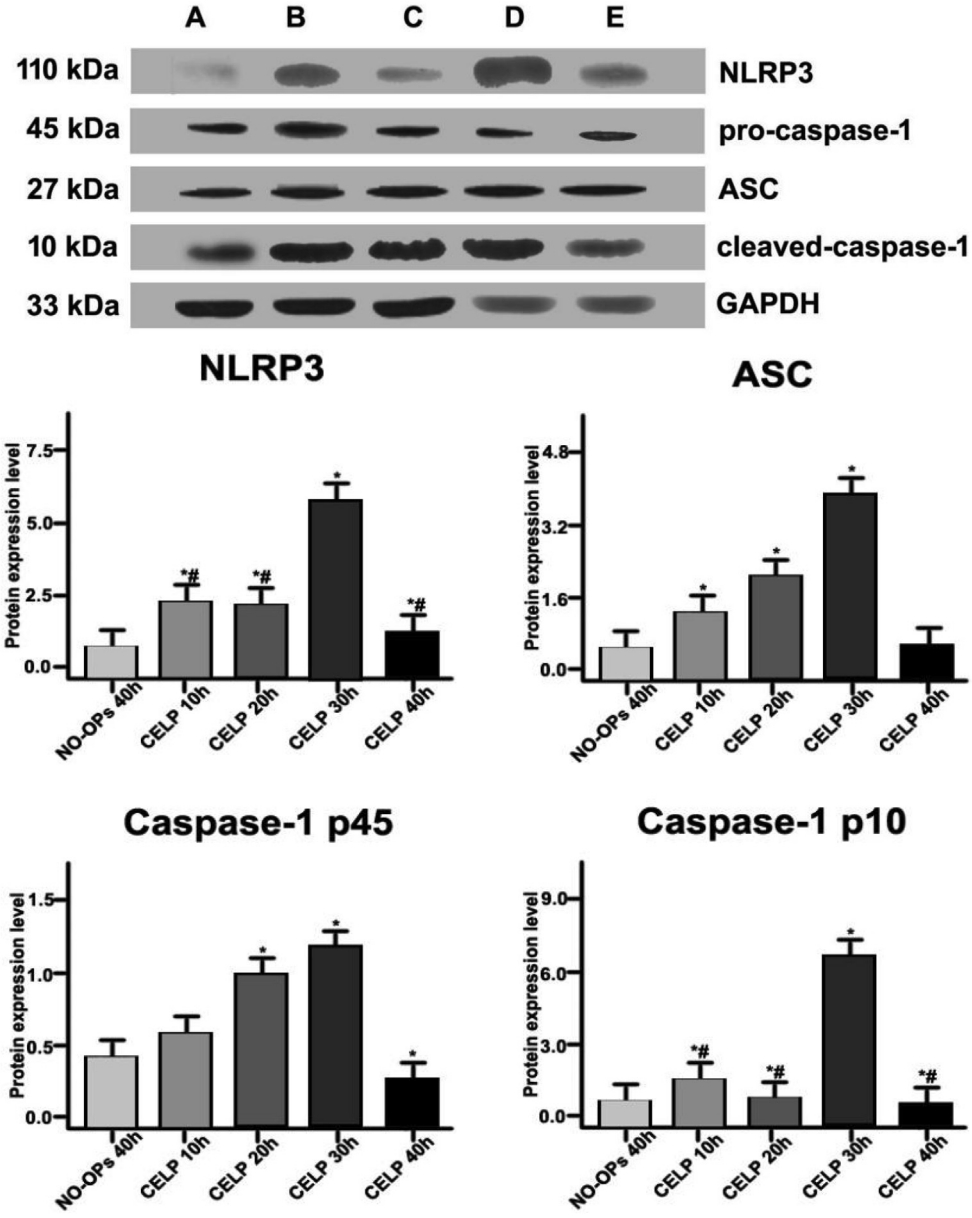

Fig. 4. Expression levels of NLRP3, ASC, Caspase-1, and IL-1β in renal tissues in each group. (A) 40 h after operation in NO-Ops group; (B) 10 h after operation in CELP group; (C) 20 h after operation in CELP group; (D) 30 h after operation in CELP group; (E) 40 h after operation in CELP group. * P < 0.05, compared with 40 h after operation in the NO-OPs group. # P < 0.05, compared with 30 h after CELP.

the expression levels of NLRP3, ASC, caspase-1 (45 kDa), and caspase-1 (10 kDa) in the renal tissue of the CELP group were increased at 10, 20, 30, and 40 h post-operation ($P < 0.05$). The expression levels of NLRP3 and caspase-1 (45/10 kDa) were significantly higher in the CELP group at 10, 20, and 40 h post-operation ($P < 0.05$).

3.5. Effects of Mito-TEMPO on HRI-induced NLRP3 inflammatory bulk signaling pathway in RTE cells

Renal tubular epithelial (RTE) cells were obtained from rats. As illustrated in Fig. 5(A) and (B), the expression levels of NLRP3, ASC, caspase-1, IL-1β, and IL-18 corresponding to the Mito-TEMPO (a mitochondria-targeted antioxidant) group were decreased ($P < 0.05$). In Fig. 5(C), the combination of Mito-TEMPO and hypoxia-reoxygenation (HRI) models revealed that the NLRP3 gene in RTE cells was distributed around the cells. The HRI model could promote the expression level of NLRP3 gene, mitochondria may aggregate around the gene, and there was a localization relationship. In addition, HRI + Mito-TEMPO could reduce the expression of NLRP3 gene and also decrease co-localization of NLRP3 with mitochondria, suggesting that Mito-TEMPO could reduce mROS, which in turn inhibited the activity of NLRP3 inflammatory bodies.

3.6. Effects of TXNIP on HRI-induced inflammatory activity of NLRP3 in RTE cells

According to the previous analysis, NLRP3 and HRI could together promote the increase of NLRP3 expression, while the activity of NLRP3 may depend on the oxygen supply of mitochondria. Mito-TEMPO could produce a large amount of mROS in order to inhibit the secretion of oxygen components and the activity of NLRP3.

Further research is required to indicate whether NLRP3 has a growth signaling pathway, except for that mROS can inhibit the secretion of oxygen components. Under hypoxia-reoxygenation conditions, RTE cells secrete TXNIP. This gene can regulate the oxygen supply process in cells, thus it is essential to explore its role in the activation of NLRP3 inflammatory bodies, as shown in Fig. 6.

In Fig. 6(A), it was observed that TXNIP was distributed in renal tubular epithelial cells, and HRI promoted its expression level. NLRP3-TXNIP and NLRP3-ASC were obtained by co-staining. Under HRI conditions, the co-localization of NLRP3-TXNIP was significantly enhanced, and the activity of NLRP3 inflammatory bodies was markedly improved, as shown in Fig. 6(B).

On the basis of HRI, Mito-TEMPO was added as a test condition, and Mito-TEMPO inhibited the expression level of TXNIP and NLRP3 (Fig. 6(C)). RTE cells were subjected to HRI operation in an immunoprecipitation experiment, and TXNIP promoted expression levels of NLRP3, as shown in Fig. 6(C). The expression level of TXNIP protein could be inhibited by siRNA transfection technology, thereby inhibiting the activation of NLRP3 inflammatory body signaling pathway, as displayed in Fig. 6(E), (F), and (G).

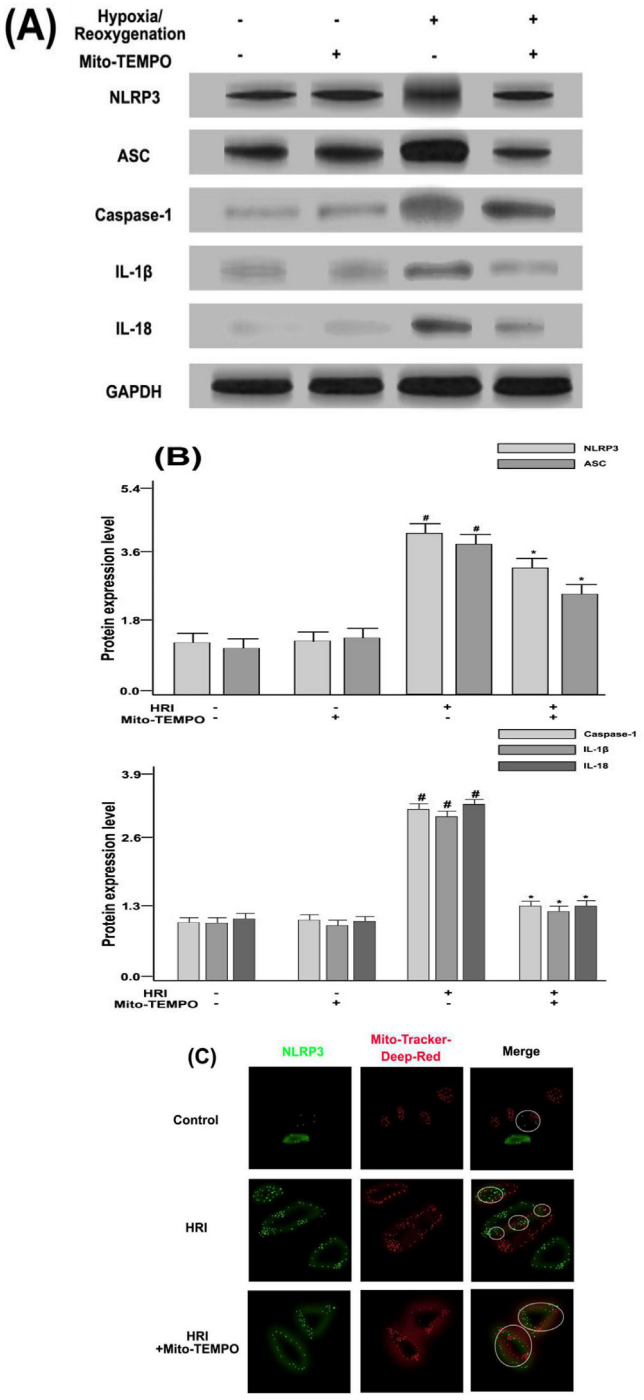

Fig. 5. (A) Expression levels of NLRP3, ASC, Caspase-1, IL-1β, and IL-18 in kidney tissues under the condition of Mito-TEMPO/HRI by Western blotting; (B) The protein content of GAPDH was used to calculate the relative expression levels of NLRP3, ASC, Caspase-1, IL-1β, and IL-18 in kidney tissues. # $P < 0.05$, compared with NO-OPs group. * $P < 0.05$, compared with HRI group. (C) Distribution of NLRP3 (green) and Mito-Tracker (red) in RTE cells could be observed by confocal microscopy.

4. Discussion

The AKI caused by sepsis is important to the pathogenesis of kidney injury. In this study, abdominal resection by surgical suture was performed to simulate the AKI model of rats. Our findings showed that a variety of cells and their signaling pathways can influence the mechanism of action of kidney injury. Among them, the signaling pathway of NLRP3 inflammatory corpuscle plays a pivotal role in the pathogenesis of renal injury diseases. NLRP3 inflammatory bodies can be activated by different substances, such as pathogen-related molecules, damage-related molecules, environmental stimuli, and pathogenic bacteria. Thus, NLRP3 differs from other inflammatory bodies. In the present study, NLRP3 inflammatory corpuscles have been found to be involved in a number of processes in kidney disease, aggravating proteinuria nephropathy.

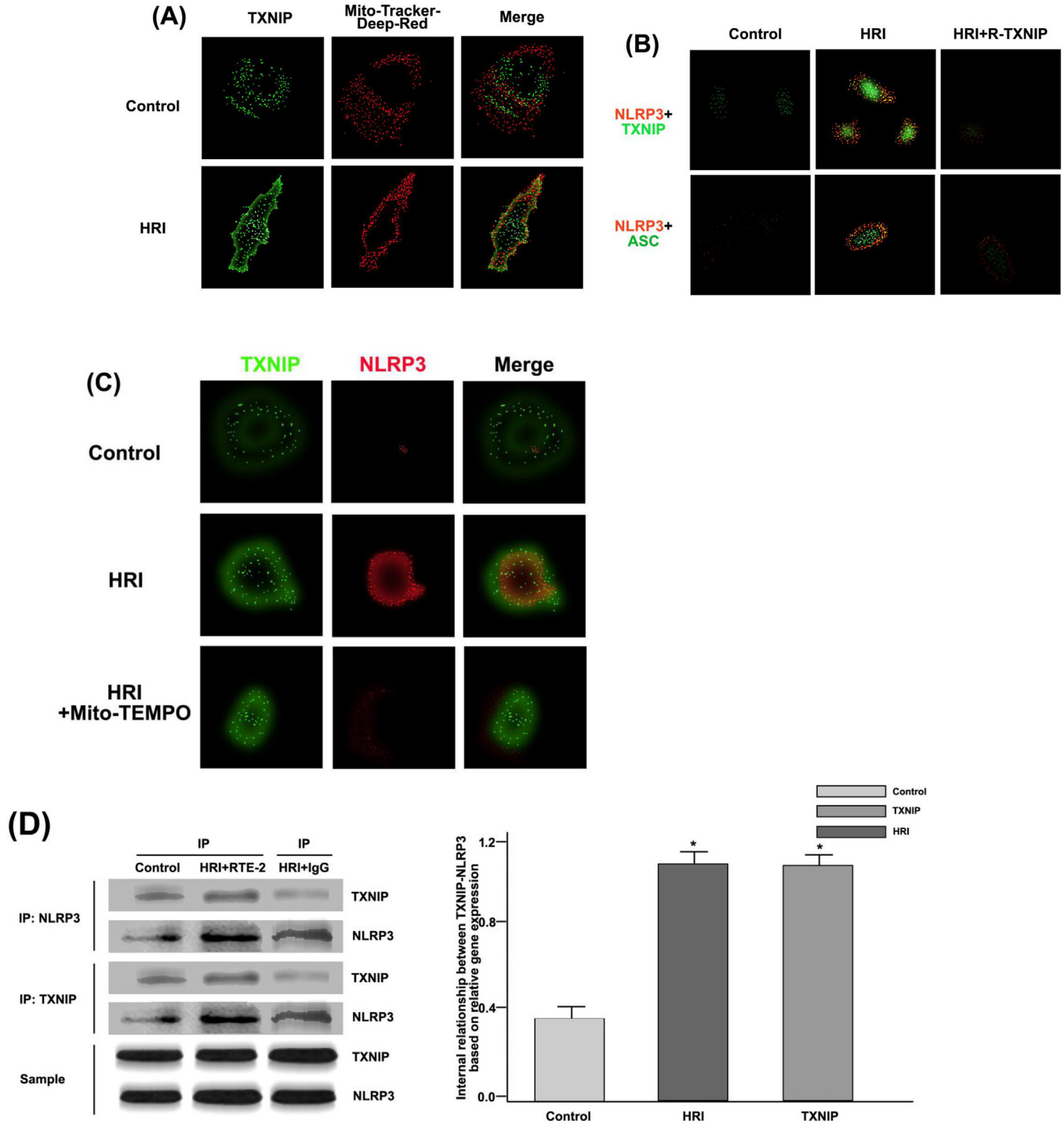

Fig. 6. TXNIP generation and TXNIP-NLRP3 were combined to modulate the activity of NLRP3 inflammatory bodies in the HRI model. (A) Distribution of TXNIP (green) and Mito-Tracker (red) in RTE cells could be observed by confocal microscopy; (B) Expression levels of NLRP3 (red) and TXNIP, ASC (green) in RTE cells could be observed by confocal microscopy. Among them, TXNIP used siRNA transfection to suppress; (C) By confocal microscopy, HRI and Mito-TEMPO were set as experimental conditions, and distribution of NLRP3 (red) and TXNIP (green) was analyzed; (D) Co-immunoprecipitation studies of NLRP3 expression were regulated by TXNIP under the HRI model. * $P < 0.05$, compared with the control group; (E) The effects of siRNA on TXNIP activation could be observed by Western blotting. # $P < 0.05$, compared with the control group; (F) HRI, single siRNA, and TXNIP + siRNA were used as experimental conditions, and the expression levels of NLRP3, ASC, Caspase-1, IL-1β, IL-18, and GAPDH in renal tissues could be observed by Western blotting; (G) GAPDH protein was used as a scale to calculate the expression levels of NLRP3, ASC, Caspase-1, IL-1β, IL-18, and GAPDH. # $P < 0.05$, compared with the control group, and * $P < 0.05$, compared with the single siRNA group.

The HRI model was established in renal tubular epithelial cells of rats, and NLRP3 was activated. Induction of TXNIP-NLRP3 activated the signaling pathway of NLRP3 inflammatory corpuscles, aggravating kidney damage, thereby inhibiting NLRP3 inflammatory bodies, as well as protecting the damaged kidney tissues. However, whether there was the recruitment of neutrophils, macrophages and other immune cells in renal injury, or whether all the up-regulated proteins related to inflammatory corpuscles came from renal tubular epithelial cells, and how NLRP3 inflammatory corpuscles converted different risk signals into the expression of pro-inflammatory factors needed further study.

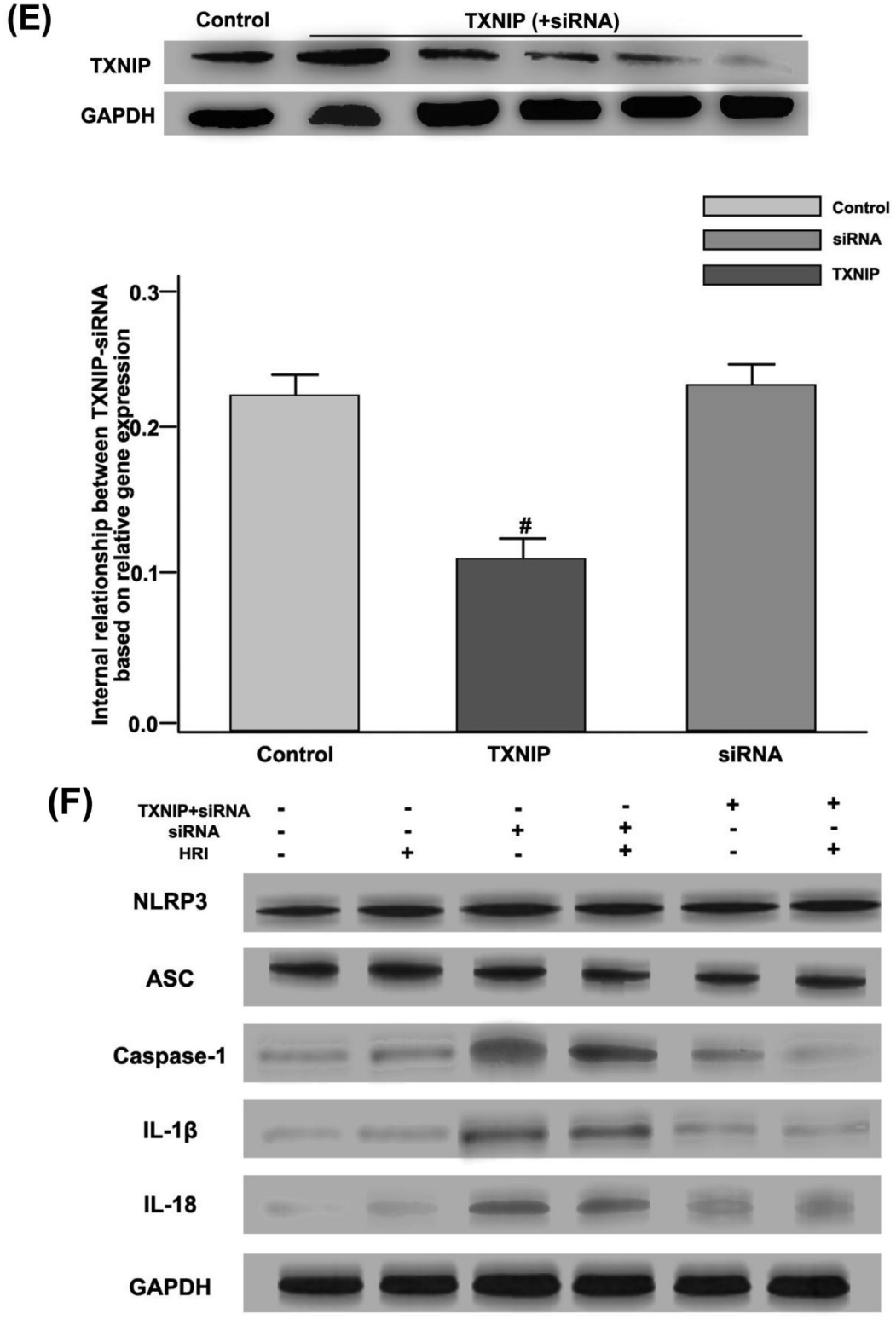

Fig. 6 (*continued*)

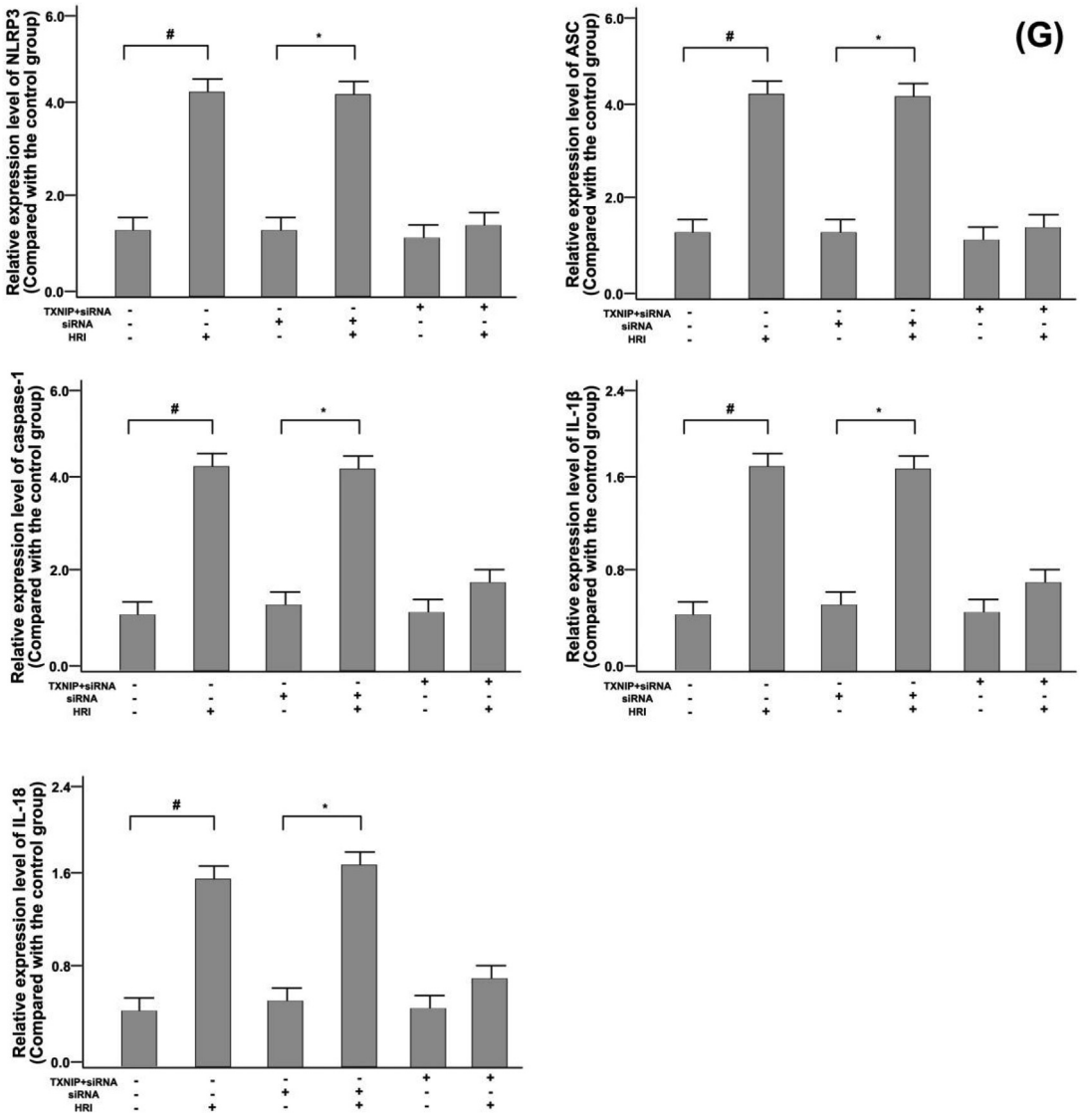

Fig. 6 (*continued*)

Declaration of Competing Interest

There is no conflict of interest.

References

Bingbing, S., Xiang, W., Zhaoxia, J., Meiying, W., Tian, Xia, 2015. Nadph oxidase-dependent nlrp3 inflammasome activation and its important role in lung fibrosis by multiwalled carbon nanotubes. Small 11 (17), 2087–2097.

Craciun, F.L., Iskander, K.N., Chiswick, E.L., Stepien, D.M., Henderson, J.M., Remick, D. G., 2014. Early murine polymicrobial sepsis predominantly causes renal injury. Shock 41 (2), 97–103.

Inna, S.A., Zhenyu, Z., Michael, K., Rudi, B., 2017. Limiting inflammation - The negative regulation of NF-B and the NLRP3 inflammasome. Nat. Immunol. 18 (8), 861–869.

Jianru, Li, Jingsen, C., Hangbo, M., Jingyin, C., Gao, C., 2015. Minocycline protects against nlrp3 inflammasome-induced inflammation and p53-associated apoptosis in early brain injury after subarachnoid hemorrhage. Mol. Neurobiol. 53 (4), 1–11.

Khwaja, Arif, 2012. Kdigo clinical practice guidelines for acute kidney injury. Nephron Clin. Pract. 120 (4), 179–184.

Mccullough, P.A., Choi, J.P., Feghali, G.A., Schussler, J.M., Stoler, R.M., Vallabahn, R.C., et al., 2016. Contrast-induced acute kidney injury. J. Am. Coll. Cardiol. 68 (13), 1465–1473.

Ostermann, M., Dickie, H., Barrett, N.A., 2012. Renal replacement therapy in critically ill patients with acute kidney injury–when to start. Nephrol. Dial. Transplant. 27 (6), 2242–2248.

Satoh, M., Tabuchi, T., Itoh, T., Nakamura, M., 2014. Nlrp3 inflammasome activation in coronary artery disease: results from prospective and randomized study of treatment with atorvastatin or rosuvastatin. Clin. Sci. 126 (3), 233–241.

Young, C.A., Ju, Y.H., Young, L.K., Sun, I.O., 2018. Clinical characteristics of sepsis-induced acute kidney injury in patients undergoing continuous renal replacement therapy. Ren. Fail. 40 (1), 403–409.

Zhang, P., Yang, Y., Lv, R., Zhang, Y., Xie, W., Chen, J., 2012. Effect of the intensity of continuous renal replacement therapy in patients with sepsis and acute kidney injury: a single-center randomized clinical trial. Nephrol. Dial. Transplant. 27 (3), 967–973.